A numerical adaptation of self-avoiding walk identities from the honeycomb to other 2D lattices

2012 J. Phys. A: Math. Theor. 45 035201

(http://iopscience.iop.org/1751-8121/45/3/035201)

J. Phys. A: Math. Theor. **45** (2012) 035201 (18pp) doi:10.1088/1751-8113/45/3/035201

A numerical adaptation of self-avoiding walk identities from the honeycomb to other 2D lattices

Nicholas R Beaton, Anthony J Guttmann and Iwan Jensen

ARC Centre of Excellence for Mathematics and Statistics of Complex Systems, Department of Mathematics and Statistics, The University of Melbourne, VIC 3010, Australia

E-mail: nbeaton@ms.unimelb.edu.au, t.guttmann@ms.unimelb.edu.au and i.jensen@ms.unimelb.edu.au

Received 25 October 2011
Published 15 December 2011
Online at stacks.iop.org/JPhysA/45/035201

Abstract
Recently, Duminil-Copin and Smirnov proved a long-standing conjecture of Nienhuis that the connective constant of self-avoiding walks (SAWs) on the honeycomb lattice is $\sqrt{2+\sqrt{2}}$. A key identity used in that proof depends on the existence of a parafermionic observable for SAWs on the honeycomb lattice. Despite the absence of a corresponding observable for SAWs on the square and triangular lattices, we show that in the limit of large lattices, some of the consequences observed on the honeycomb lattice persist on other lattices. This permits the accurate estimation, though not an exact evaluation, of certain critical amplitudes, as well as critical points, for these lattices. For the honeycomb lattice, an exact amplitude for loops is proved.

PACS numbers: 05.50.+q, 05.10.−a

(Some figures may appear in colour only in the online journal)

1. Introduction

In 2010, Duminil-Copin and Smirnov [6] proved that the critical point of honeycomb lattice self-avoiding walks (SAWs) is $z_c = 1/\sqrt{2+\sqrt{2}}$, as conjectured by Nienhuis [17]. Their proof rested on establishing a connection between three generating functions for walks in a regular trapezoidal sublattice $S_{T,L}$ of the honeycomb lattice, as shown in figure 1, of width T and left-height $2L$. All walks start on the half-edge a incident on the left wall labelled α.

They first identified a parafermionic observable:

$$F(x) = \sum_{\omega \subset S: a \to x} \mathrm{e}^{-\mathrm{i}\sigma W_\omega(a,x)} z^{l(\omega)}.$$

Here, x is a point (specifically, the mid-point between two adjacent vertices) in the domain, $\sigma \in \mathbb{R}$, $z \geqslant 0$, and ω is a path starting at half-edge a and finishing at point x. $l(\omega)$ is the length of the path and $W_\omega(a, x)$ is the winding, or total rotation in radians, when ω is traversed from a to x.

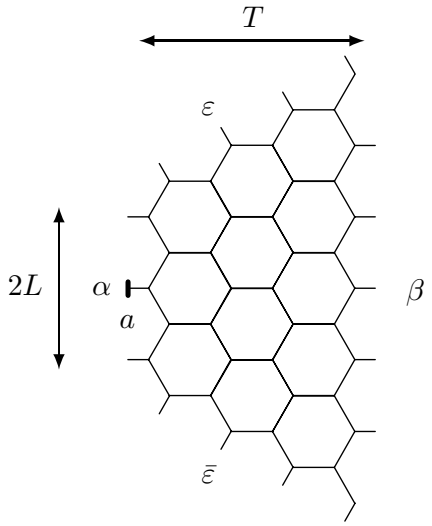

Figure 1. Finite patch $S_{3,1}$ of the honeycomb lattice. Paths run from mid-edge to mid-edge acquiring a weight z for each step. The paths start on the central mid-edge of the left boundary (shown as a).

In the special case $z = z_c = 1/\sqrt{2+\sqrt{2}}$ and $\sigma = 5/8$, F satisfies half of the discrete Cauchy–Riemann equations [19],

$$(p - v)F(p) + (y - v)F(q) + (r - v)F(r) = 0, \tag{1}$$

where p, q, r are the mid-edges of the three edges incident on vertex v.

By summing (1) over all vertices in $S_{T,L}$, contributions from interior mid-edges cancel and we are left with a relation involving only mid-edges on the boundary of $S_{T,L}$. Walks from half-edge a to the boundary fall into three classes, depending on which boundary edge they terminate at. This observation gives rise to the following three generating functions:

$$A_{T,L}(z) := \sum_{\substack{\gamma \subset S_{T,L} \\ a \to \alpha/\{a\}}} z^{\ell(\gamma)},$$

$$B_{T,L}(z) := \sum_{\substack{\gamma \subset S_{T,L} \\ a \to \beta}} z^{\ell(\gamma)},$$

$$E_{T,L}(z) := \sum_{\substack{\gamma \subset S_{T,L} \\ a \to \varepsilon \cup \bar{\varepsilon}}} z^{\ell(\gamma)},$$

where the sums are over all self-avoiding walks from a to the α, β or $\varepsilon, \bar{\varepsilon}$ boundaries, respectively.

Duminil-Copin and Smirnov showed that the relation involving boundary mid-edges can be written in the form

$$1 = \cos\left(\frac{3\pi}{8}\right) A_{T,L}(z_c) + \cos\left(\frac{\pi}{4}\right) E_{T,L}(z_c) + B_{T,L}(z_c). \tag{2}$$

Taking the limit $L \to \infty$, this becomes

$$1 = \cos\left(\frac{3\pi}{8}\right) A_T(z_c) + \cos\left(\frac{\pi}{4}\right) E_T(z_c) + B_T(z_c). \tag{3}$$

This is now a relation linking three generating functions for SAWs in a strip of width T. Duminil-Copin and Smirnov then used this to prove Nienhuis's conjecture.

In [2], it was proved that $E_T(z_c) = 0$, so (3) can in fact be simplified to

$$1 = \cos\left(\frac{3\pi}{8}\right) A_T(z_c) + B_T(z_c). \tag{4}$$

This modification slightly simplifies the proof of Duminil-Copin and Smirnov.

This simpler identity, involving just two generating functions, raises the question as to its applicability to other two-dimensional lattices, such as the square and triangular lattices. However, it should be remarked that the critical points are not known exactly for these lattices, though high precision numerical estimates are available. The proof of Duminil-Copin and Smirnov identifying the critical point cannot be repeated for these lattices, as there is no known appropriate parafermionic observable satisfying an identity like (1). As shown by Ikhlef and Cardy [10], the dilute O(n) model on the square lattice does have a parafermionic observable, and this can be used to identify its critical point. In the $n \to 0$ limit, however, that model is not the usual SAW model. For the triangular lattice we know of no appropriate parafermionic observable.

However, leaving aside considerations of discrete holomorphicity and the existence of parafermions, and motivated by a more detailed study of the width (T) dependence of the two generating functions $A_T(z)$ and $B_T(z)$, we investigated which features of the identity (4) carry over to other two-dimensional lattices.

We did this by calculating data for the generating functions $A_T(z)$ and $B_T(z)$ in strips, for $T \leqslant 10$ on the honeycomb lattice, for $T \leqslant 15$ on the square lattice and for $T \leqslant 11$ on the triangular lattice. In figure 2, we show a plot of $\cos(3\pi/8)A_T(z) + B_T(z)$ for $T \in [1, \ldots, 10]$, on the honeycomb lattice, showing the intersection of all curves at $(z_c, 1)$, as expected from (4).

When we repeated this calculation using the square and triangular lattice data, we found that there was no unique point of intersection, though the discrepancy was too small to be visible on a plot such as figure 2. Instead we observed a definite monotonic width dependence, described in greater detail below. We first investigated a more general form of (4), allowing the 'constants' to be width dependent. That is to say, we assumed

$$1 = c_\alpha(T)A_T(z_c) + c_\beta(T)B_T(z_c).$$

We fitted successive pairs of points $(A_T(z_c), B_T(z_c))$ and $(A_{T+1}(z_c), B_{T+1}(z_c))$ in order to estimate $c_\alpha(T)$ and $c_\beta(T)$ and found a weak T dependence in both 'constants'. More significantly, however, we conjecture that

$$\lim_{T\to\infty} c_\alpha(T)/c_\beta(T) = \cos(3\pi/8),$$

just as in the honeycomb lattice case, based on agreement to more than five significant digits for both the square and the triangular lattices. In hindsight, this is perhaps not too surprising, as the constants multiplying the two generating functions arise from the winding angle of contributing graphs, and these are independent of lattice for the two generating functions considered, being $\pm\pi$ rad for $A(z)$ and 0 for $B(z)$.

Assuming that this ratio is indeed $\cos(3\pi/8)$ for all lattices, we re-analysed the data with this assumption implicit. That is to say, we fitted the data to

$$c(T) = \cos(3\pi/8)A_T(z_c) + B_T(z_c).$$

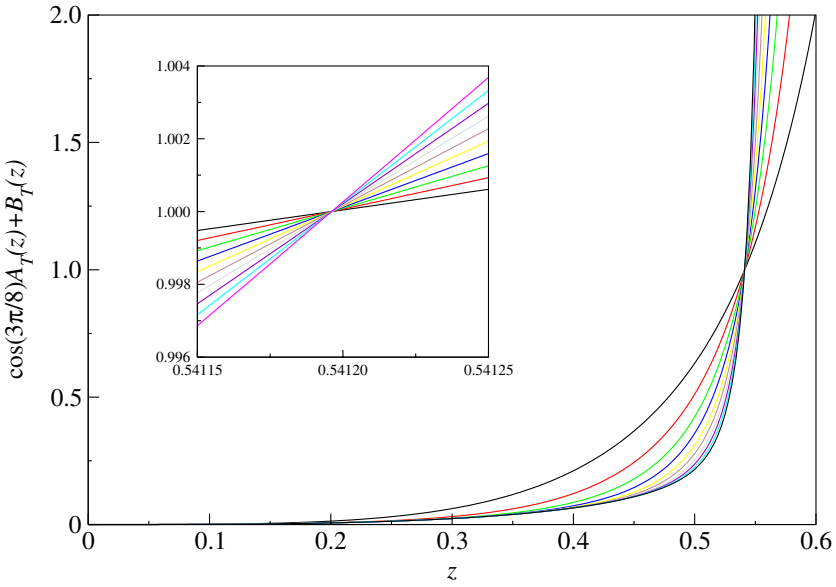

Figure 2. Plot of $\cos(3\pi/8)A_T(z)+B_T(z)$ for $T \in [1, \ldots, 10]$, for the honeycomb lattice, showing interception of all curves at $(z_c, 1)$. The inset shows a close-up of the region of interception.

We were able to estimate both the limit $\lim_{T\to\infty} c(T)$, which is of course lattice dependent, and also the nature of the T dependence. Putting all this together, we estimated for the square lattice

$$1.024\,966(1 - 0.14/T^2) \approx \cos(3\pi/8)A_T(z_c) + B_T(z_c). \tag{5}$$

For the triangular lattice, the corresponding result is

$$1.901\,979(1 - 0.1/T^2) \approx \cos(3\pi/8)A_T(z_c) + B_T(z_c). \tag{6}$$

The leading constant is expected to be sufficiently accurate so as to restrict errors to one or two places in the last quoted digit. The correction term is given as $O(1/T^2)$ but that exponent is a guess based an a numerical estimate in the range $(1.9, 2.1)$. Finally, the magnitude of that term is claimed to be accurate only to 10–20%.

This limiting behaviour as $T \to \infty$ suggests a new numerical method for estimating the critical point. For the honeycomb lattice, the intersection point of $\cos(3\pi/8)A_T(z)+B_T(z)$ for any two distinct values of T uniquely determines z_c. For the square and triangular lattices, we instead looked at the intersection point of $\cos(3\pi/8)A_T(z) + B_T(z)$ and $\cos(3\pi/8)A_{T+1}(z) + B_{T+1}(z)$. Call this intersection point $z_c(T)$. Then, one expects $\lim_{T\to\infty} z_c(T) = z_c$.

In this way, we estimated

$$z_c = 0.379\,052\,2775 \pm 0.000\,000\,0005$$

for the square lattice and

$$z_c = 0.240\,917\,572 \pm 0.000\,000\,005$$

for the triangular lattice. These estimates can be compared to the best series estimates, based on the analysis of very long polygon series, which are $z_c(\text{sq}) = 0.379\,052\,277\,76$ [11, 12], with uncertainty in the last digit, and $z_c(\text{tr}) = 0.240\,917\,5745$ [14], with the similar uncertainty.

Another result proved by Beaton, de Gier and Guttmann [2] is that $\lim_{T\to\infty} B_T(z) = B(z) = 0$ for $z \leqslant z_c$. This means that, in this limit, the identity (4) further simplifies to

$$1 = \cos(3\pi/8)A(z_c), \tag{7}$$

where $A(z) = \lim_{T\to\infty} A_T(z)$. Now $A(z)$ is the generating function for loops (half-plane walks which begin and end on the boundary), which is expected to behave [9] as

$$A(z) \sim a_0 + a_1(1 - z/z_c)^{3/16},$$

so (7) implies an *exact* value for the critical amplitude:

$$a_0 = 1/\cos(3\pi/8).$$

Correspondingly, highly accurate predictions for this amplitude for the square and triangular lattices follow from (5) and (6), notably

$$a_0(\mathrm{sq}) \approx 1.024\,966/\cos(3\pi/8) = 2.678\,365$$

and

$$a_0(\mathrm{tr}) \approx 1.901\,979/\cos(3\pi/8) = 4.970\,111.$$

We remark that, as discussed below, we have normalized these generating functions differently for these two lattices, so please note details of the normalization before using these estimates.

Finally, we studied the behaviour of the two generating functions as $T \to \infty$. We found $B_T(z) \sim \mathrm{const}/T^{\alpha}$, where $\alpha \approx 0.25$. This is precisely as predicted in [6], based on conjectures of Lawler *et al* [15] as to the number of SAWs on the boundary of a domain. In [6], it was pointed out that the conjecture implies that $B_T(z_c)$ should decay as $T^{-1/4}$ as T goes to infinity, just as we observed.

Similarly, we can investigate how $\tilde{A}_T(z_c) = A_T(z_c) - a_0$ decays as T tends to infinity. From (4) it follows that $\tilde{A}_T(z_c)$ also decays like $T^{-1/4}$ and this was observed numerically.

2. Honeycomb lattice

The original identity of Duminil-Copin and Smirnov related three distinct generating functions for SAWs in a finite domain. Letting the length L of the domain become unbounded changes the domain into a strip of finite width T. As proved in [2], the generating function $E_T(z)$ vanishes identically in that limit, so one has an identity relating two generating functions:

$$1 = \cos(3\pi/8)A_T(z_c) + B_T(z_c). \tag{8}$$

The generating functions $A_T(z)$ and $B_T(z)$ for T finite are rational. For example,

$$A_0(z) = \frac{2z^3}{1-z^2}, \qquad B_0(z) = \frac{2z^2}{1-z^2},$$

$$A_1(z) = \frac{2z^3\left(1 - z^2 + z^4 + 3z^6 - 4z^8 + z^{12}\right)}{\left(1-z^4\right)^2\left(1 - 2z^2 + z^4 - z^6\right)},$$

$$B_1(z) = \frac{2z^4\left(2 - 4z^4 + 2z^6 + 2z^8 - z^{10}\right)}{\left(1-z^4\right)^2\left(1 - 2z^2 + z^4 - z^6\right)},$$

$$A_2(z) = \frac{P_2^{\mathrm{A}}(z)}{Q_2(z)}, \qquad B_2(z) = \frac{P_2^{\mathrm{B}}(z)}{Q_2(z)}, \qquad \text{where}$$

$$P_2^{\mathrm{A}}(z) = 2(z^3 - 4z^5 + 7z^7 - 7z^9 + 9z^{11} + 2z^{13} - 31z^{15} + 39z^{17} - 46z^{19} + 68z^{21} - 75z^{23} + 74z^{25} - 61z^{27} + 41z^{29} - 20z^{31} + z^{33} + 6z^{35} - 4z^{37} + z^{39}),$$

$$P_2^{\mathrm{B}}(z) = 2z^6(1 - z^2)(4 - 4z^2 - 8z^4 + 8z^6 - 4z^8 + 16z^{10} - 12z^{12} + 18z^{14} - 10z^{16} + 3z^{18} - 3z^{20} - 4z^{22} + 10z^{24} - 10z^{26} + 5z^{28} - z^{30}),$$

$$Q_2(z) = (1 - z^2 - z^4 + z^6 - z^8)^2 \times (1 - 3z^2 + 3z^4 - 5z^6 + 8z^8 - 9z^{10} + 7z^{12} - 8z^{14} + 8z^{16} - 5z^{18} + 3z^{20} - z^{22}).$$

These generating functions have simple poles, the dominant pole being at $z = z_c(T) > z_c(T+1) > z_c$. Furthermore, $\lim_{T\to\infty} z_c(T) = z_c$ [18].

Duminil-Copin and Smirnov proved that the unique solution of

$$\cos(3\pi/8)A_T(z) + B_T(z) = 1, \tag{9}$$

for any $T \geqslant 0$, occurs at $z = z_c = 1/\sqrt{2+\sqrt{2}}$. It follows then that we could work backwards: given only the simple rational generating functions $A_0(z)$ and $B_0(z)$, we could identify the exact value of z_c simply by seeking the solution of

$$\cos(3\pi/8)A_0(z) + B_0(z) = 1.$$

If we did not already know z_c, this would be a particularly simple way to find it.

In a further demonstration of this invariant, we show in figure 2 a plot of $\cos(3\pi/8)A_T(z) + B_T(z)$ for $T \in [1, \ldots, 10]$, where it can be seen that the curves intersect at $(z_c, 1)$, in accordance with the identity (8).

Let us assume that we did not even know the Duminil-Copin and Smirnov identity (8), but rather just conjectured that some linear combination of $A_T(z_c)$ and $B_T(z_c)$ was invariant. We write this invariant as $\lambda A_T(z_c) + B_T(z_c)$. Then, by seeking the solutions, for $z > 0$, $\lambda > 0$ of the equations

$$\lambda A_0(z) + B_0(z) - \lambda A_1(z) - B_1(z) = 0$$

and

$$\lambda A_2(z) + B_2(z) - \lambda A_1(z) - B_1(z) = 0,$$

we could discover both the invariant and the exact value of the critical point from the exact solutions for strips of width 0, 1 and 2 given above.

As we show below, this suggests a way to *approximate* z_c for other lattices by similar means. We first show that, for other lattices, an appropriate linear combination of $A_T(z)$ and $B_T(z)$ approaches a limit as $T \to \infty$ and use this observation to estimate the critical point for the square and triangular lattices.

Letting the width go to infinity, another of the generating functions, $B(z)$, vanishes [2], and the identity reduces to $A(z_c) = 1/\cos(3\pi/8)$. Recall that $A(z)$ is the generating function for loops whose asymptotic behaviour is believed to be [9]

$$A(z) \sim a_0 + a_1(1 - z/z_c)^{3/16}.$$

Thus, the Duminil-Copin–Smirnov identity in the limit $L \to \infty$ and $T \to \infty$ gives us the exact value for the amplitude term $a_0 = A(z_c)$ for the honeycomb lattice.

Next we consider the behaviour of the generating functions $A_T(z)$ and $B_T(z)$ in the limit $T \to \infty$. Denote $\lim_{T\to\infty} B_T(z)$ by $B(z)$, with a similar definition of $A(z)$. Recall that, as

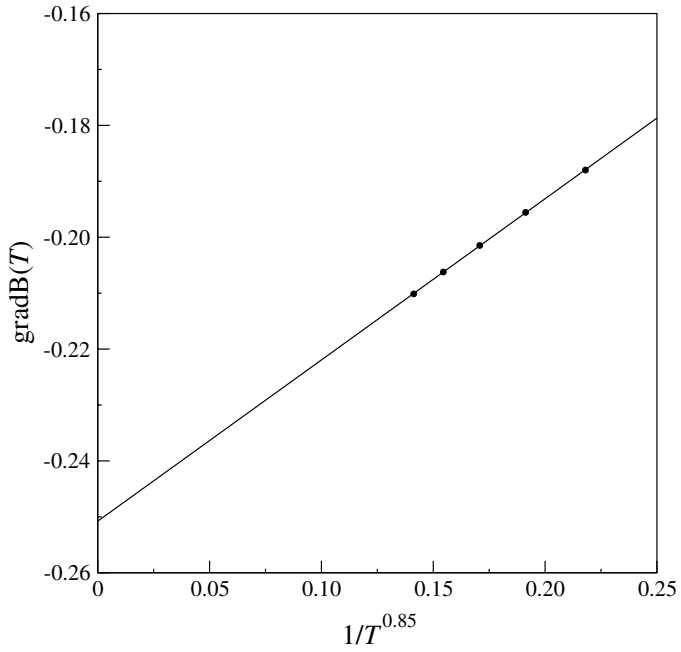

Figure 3. Plot of the local gradient of $B_T(z_c)$ and T against $1/T^{0.85}$. The straight line denotes a linear fit to the data in the plot.

proved in [2], $B(z) = 0$ for $z \leqslant z_c$. We then wish to understand exactly how $B_T(z_c) \to 0$ as $T \to \infty$.

If $B_T(z_c) \sim \text{const}/T^{\alpha}$, a log–log plot of $B_T(z_c)$ against T should be linear with the slope $-\alpha$ as $T \to \infty$. We only have data for the width $T \leqslant 10$; so the gradient is still changing slightly with T in that plot. To accommodate this, we extrapolate estimates of the local gradient. We define the local gradient as

$$\text{gradB}(T) = \log\left(\frac{B_T(z_c)}{B_{T-1}(z_c)}\right) \Big/ \log\left(\frac{T}{T-1}\right)$$

and plot grad$B(T)$ against $1/T^{0.85}$, where the exponent 0.85 was chosen empirically to make the plot linear. The plot is shown in figure 3, and it is manifestly clear that the locus extrapolates to a value of $\alpha \approx 1/4$. More systematic numerical extrapolation techniques [8] (not detailed here) lend support to this estimate. This is precisely as predicted [6], based on conjectures of Lawler, Schramm and Werner [15] as to the number of SAWs on the boundary of a domain. This is discussed in [6], where it is pointed out that the conjecture implies that $B_T(z_c)$ should decay as $T^{-1/4}$ as T goes to infinity, just as we observe.

From (8), it follows that if $B_T(z_c) \sim c/T^{1/4}$, then $\tilde{A}_T(z_c) = A_T(z_c) - a_0$ also decays as $T^{-1/4}$, and this was observed numerically by a similar plot to that described in the preceding paragraph.

3. Square lattice

As discussed above, there is no parafermionic operator that applies to the SAW model on the square lattice or the triangular lattice, so we cannot identify the critical point for SAWs on

Table 1. The values of $A_T(z)$ and $B_T(z)$ at the critical point $z = z_c$.

T	$A_T(z_c)$	$B_T(z_c)$
1	0.684 928 096 008 073	0.760 082 094 484 555
2	0.825 972 541 624 066	0.707 257 323 612 670
3	0.927 565 166 390 104	0.668 934 606 497 192
4	1.006 072 923 950 508	0.639 202 723 889 591
5	1.069 537 792 384 553	0.615 108 345 881 821
6	1.122 482 001 562 161	0.594 974 760 428 940
7	1.167 689 112 421 950	0.577 763 265 643 123
8	1.206 987 841 982 332	0.562 788 338 725 227
9	1.241 640 411 741 764	0.549 575 210 877 016
10	1.272 552 495 675 558	0.537 782 341 996 967
11	1.300 394 615 482 380	0.527 156 358 502 502
12	1.325 676 196 007 041	0.517 504 450 137 522
13	1.348 792 763 213 512	0.508 676 719 252 903
14	1.370 057 142 972 426	0.500 554 481 834 765
15	1.389 720 731 591 218	0.493 042 273 647 721

these lattices as Duminil-Copin and Smirnov did for honeycomb SAWs. We might, however, expect that in the limit $L \to \infty$ (so that we are again considering SAWs in a strip) there should be a similar relationship between the two generating functions $A_T(z)$ and $B_T(z)$, with some T dependence that vanishes as $T \to \infty$.

That is to say, while the relationship

$$1 = \cos(3\pi/8)A_T(z_c) + B_T(z_c),$$

which is an identity for honeycomb lattice SAWs for a finite width T, cannot be expected to hold for the square and triangular lattices, we might expect something like

$$1 = c_\alpha(T)A_T(z_c) + c_\beta(T)B_T(z_c)$$

to hold, where the 'constants' $c_\alpha(T)$ and $c_\beta(T)$ are weakly T dependent.

We have computed data for the square lattice generating functions in strips of width T, that is, $A_T(z)$ and $B_T(z)$, for $T \leqslant 15$, and used our best estimate $1/z_c = 2.638\,158\,530\,31$ [11, 12] to tabulate $A_T(z_c)$ and $B_T(z_c)$, shown in table 1. In [6] these generating functions for the honeycomb lattice were defined to include an extra half-step at the beginning of the walk and at the end of the walk. This introduces an extra factor of z (or, as appropriate z_c) and we have used this definition of the generating functions $A_T(z)$ and $B_T(z)$ for the square lattice data.

We then fitted successive pairs of values $(A_T(z_c), B_T(z_c))$ and $(A_{T+1}(z_c), B_{T+1}(z_c))$ for $T = 1, \ldots, 14$ to

$$1 = c_\alpha(T)A_T(z_c) + c_\beta(T)B_T(z_c)$$

and solved the associated linear equations for $c_\alpha(T)$ and $c_\beta(T)$, using our best estimate of z_c. In figures 4 and 5, we show plots of values of $c_\alpha(T)$ against $1/T^{1.15}$ and $c_\beta(T)$ against $1/T^{0.85}$.

We have no basis for assuming that this is the correct form we should choose to extrapolate these plots; rather, the T dependence was chosen experimentally to give a linear plot. Extrapolated to $T = \infty$, we find $c_\alpha \approx 0.3734$ and $c_\beta \approx 0.9756$. To obtain more precise estimates, we extrapolated these sequences using the Bulirsch–Stoer algorithm [3]. This algorithm requires a parameter w which can be thought of as a correction-to-scaling exponent. For the purpose of the current exercise, we have set this parameter to 1, corresponding to an analytic correction, which is appropriate for the two-dimensional SAW problem [4].

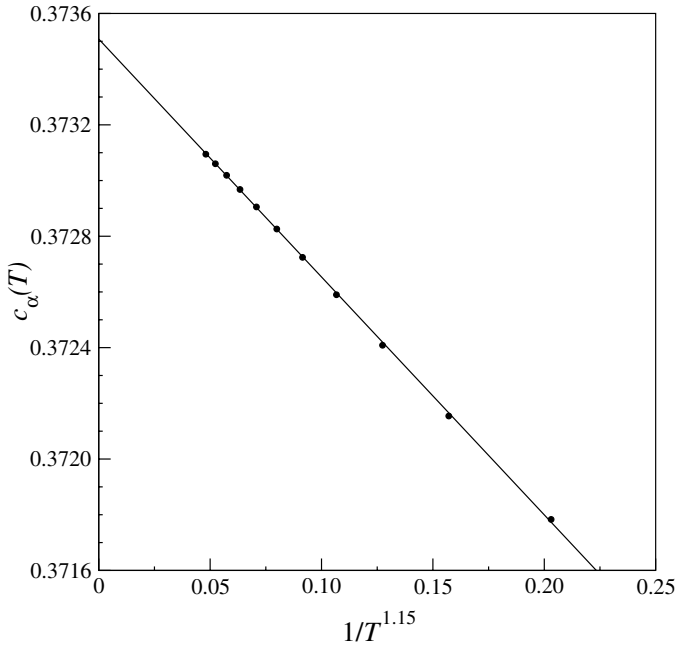

Figure 4. Plot of $c_\alpha(T)$ against $1/T^{1.15}$ for square lattice A walks. The straight line denotes a linear fit to the last seven data points in the plot.

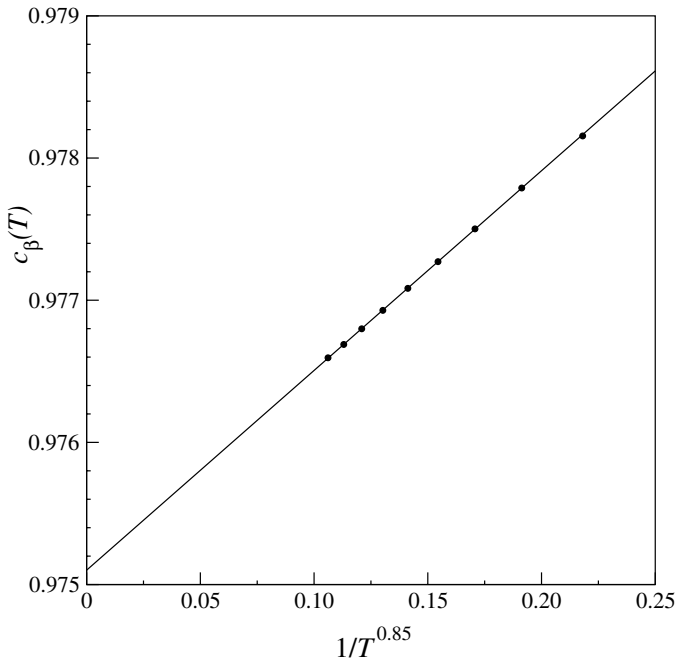

Figure 5. Plot of $c_\beta(T)$ against $1/T^{0.85}$ for square lattice B walks. The straight line denotes a linear fit to the last seven data points in the plot.

Our implementation of the algorithm is precisely as described by Monroe [16], and we retained 40 digit precision throughout. We also applied a range of standard extrapolation algorithms to the sequences $\{c_\alpha(T)\}$ and $\{c_\beta(T)\}$. These were Levin's u-transform, Brezinski's θ algorithm, Neville tables, Wynn's ϵ algorithm and the Barber–Hamer algorithm [1]. Descriptions of these algorithms, and codes for their implementation, can be found in [8]. These gave results totally consistent with, but less precise than, those from the Bulirsch–Stoer algorithm.

In this way, we estimated $c_\alpha = 0.373\,362 \pm 0.000\,001$ and $c_\beta = 0.975\,644 \pm 0.000\,002$. Thus the ratio $c_\alpha/c_\beta = 0.382\,683(2)$. For the honeycomb lattice the corresponding ratio is $\cos(3\pi/8) = 0.382\,6834\ldots$, which is close to, and probably equal to, the square lattice value. We shall see in the next section that this apparent agreement also holds for the triangular lattice.

Assuming that $c_\alpha/c_\beta = \cos(3\pi/8)$ for the square lattice, we calculated elements of the sequence $\cos(3\pi/8)A_T(z_c) + B_T(z_c)$ and extrapolated these using the same extrapolation method as described above. We found the limit of the sequence to be $1.024\,966 \pm 0.000\,001$, compared to a value of exactly 1 for the honeycomb lattice. Using this estimate, we plotted $\log(\cos(3\pi/8)A_T(z_c) + B_T(z_c) - 1.024\,966)$ against $\log T$. The plot displayed slight curvature; so we plotted the local gradient

$$\log\left(\frac{\cos(3\pi/8)A_T(z_c) + B_T(z_c) - 1.024\,966}{\cos(3\pi/8)A_{T-1}(z_c) + B_{T-1}(z_c) - 1.024\,966}\right) \Big/ \log\left(\frac{T}{T-1}\right)$$

against $1/T$. This extrapolated to a value in the range $(1.9, 2.1)$; so we took the central value and concluded that $1.024\,966 - \frac{c_1}{T^2} \approx \cos(3\pi/8)A_T(z_c) + B_T(z_c)$ is the asymptotic behaviour. Finally, extrapolating estimates of the constant c_1, we estimate $c_1 \approx 0.14 \pm 0.02$. Our final result is

$$1.024\,966 - \frac{0.14}{T^2} \approx \cos(3\pi/8)A_T(z_c) + B_T(z_c),$$

which is an accurate mnemonic for square lattice strips.

For the honeycomb lattice, it has been proved [2] that $\lim_{T\to\infty} B_T(z_c) = B(z_c) = 0$. The proof applies *mutatis mutandis* to the square and triangular lattices. Thus in the limit of infinite strip width we find $1 \approx 0.373\,3621A(z_c)$, giving a prediction for the critical amplitude $A(z_c) \approx 2.678\,365$. Current series estimates (unpublished) are 2.66 ± 0.03, some four orders of magnitude less accurate than this new estimate.

For the honeycomb lattice, the intersection point of $\cos(3\pi/8)A_T(z) + B_T(z)$ for any two distinct values of T uniquely determines z_c. For the square and triangular lattices, we instead looked at the intersection point of $\cos(3\pi/8)A_T(z) + B_T(z)$ and $\cos(3\pi/8)A_{T+1}(z) + B_{T+1}(z)$. Call this intersection point $z_c(T)$. Then, one expects $\lim_{T\to\infty} z_c(T) = z_c$. We extrapolated the sequence $\{z_c(T)\}$ using the same Bulirsch–Stoer method described above, and in this way, we estimated

$$z_c = 0.379\,052\,2775 \pm 0.000\,000\,0005.$$

This estimate can be compared to the best series estimates, based on the analysis of very long polygon series, $z_c(\mathrm{sq}) = 0.379\,052\,277\,76$ [11, 12], with uncertainty in the last digit. Thus, this method is seen to be a powerful new method for estimating critical points, giving very good accuracy, though it does not rival the most powerful methods based on the series analysis of polygon series. However, it does give comparable accuracy to methods based on the series analysis of SAWs (rather than self-avoiding polygons (SAPs)).

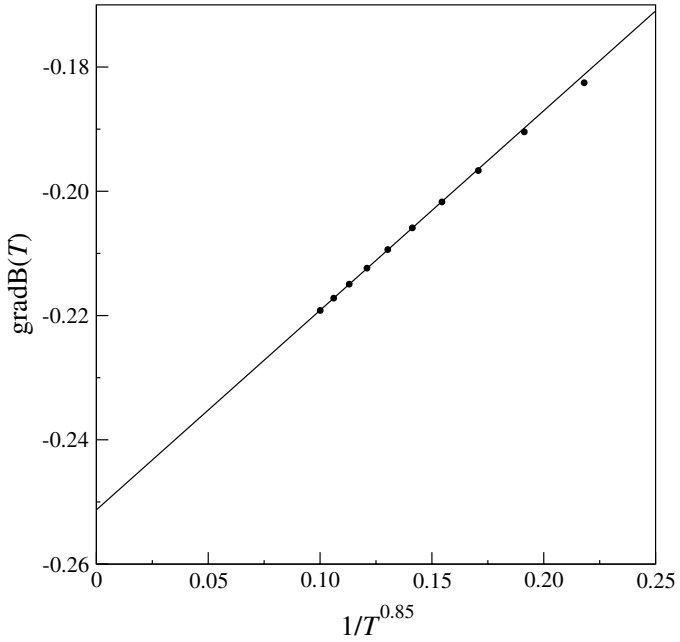

Figure 6. Plot of grad$B(T)$ against $1/T^{0.85}$ for square lattice B walks. The straight line denotes a linear fit to the last seven data points in the plot. Linear extrapolation to -0.25 is well supported.

3.1. T dependence of the generating functions $A_T(z_c)$ and $B_T(z_c)$

As for the honeycomb lattice, we expect $B_T(z_c) \sim \text{const}/T^{1/4}$. In figure 6, we have plotted estimates of the exponent

$$\text{grad}B(T) = \log\left(\frac{B_T(z_c)}{B_{T-1}(z_c)}\right) \Big/ \log\left(\frac{T}{T-1}\right)$$

against $1/T^{0.85}$. This local gradient should approach $-1/4$ and from the plot is seen to do so.

As for the honeycomb lattice, from (8) it follows that if $B_T(z_c) \sim \text{const}/T^{1/4}$, then $\tilde{A}_T(z_c) = A_T(z_c) - a_0$ also decays as $T^{-1/4}$. This was observed numerically by a similar plot to that described in the preceding paragraph.

3.2. Alternative estimate of the critical point

We showed in section 2 that the critical point could be identified just from knowledge of the invariant (8) and the formulae for $A_0(z)$ and $B_0(z)$. In the case of the square lattice, we expect the simultaneous solution of the pair of equations

$$\lambda A_{T-1}(z) + B_{T-1}(z) - \lambda A_T(z) - B_T(z) = 0$$

and

$$\lambda A_T(z) + B_T(z) - \lambda A_{T+1}(z) - B_{T+1}(z) = 0$$

to give a sequence of estimates of $z_c(T)$ that should converge to the critical point z_c. Similarly, the parameter λ should converge to the ratio $c_\alpha/c_\beta = \cos(3\pi/8)$. The merit of this method of estimating the critical point is that it makes no assumption about the value of λ, while the method of estimating the critical point described in section 3 assumes that $\lambda = \cos(3\pi/8)$.

Table 2. Estimates of $z_c(T)$ and $\lambda(T)$ for the square lattice.

T	$z_c(T)$	$\lambda(T)$
2	0.379 213 251 099 6564	0.368 086 501 616 0631
3	0.379 135 427 580 2486	0.372 495 704 364 6600
4	0.379 101 458 721 2902	0.375 032 777 979 0171
5	0.379 083 764 984 1775	0.376 692 160 796 3391
6	0.379 073 617 716 1640	0.377 847 366 551 0655
7	0.379 067 389 603 7665	0.378 686 839 260 6266
8	0.379 063 360 259 6354	0.379 317 622 909 3515
9	0.379 060 640 619 0476	0.379 804 622 288 1576
10	0.379 058 739 886 2656	0.380 189 141 544 0993
11	0.379 057 372 178 2793	0.380 498 524 927 9112
12	0.379 056 363 351 5162	0.380 751 485 962 1669
13	0.379 055 603 233 4455	0.380 961 199 086 9139
14	0.379 055 019 822 686	0.381 137 168 185 8631

Table 3. Estimates of $A_T(z_c)$ and $B_T(z_c)$ for various strip widths for the triangular lattice.

T	$A_T(z_c)$	$B_T(z_c)$
1	1.139 480 549 210 468	1.457 161 363 236 105
2	1.435 344 242 350 752	1.348 134 252 648 887
3	1.641 756 149 326 264	1.270 897 362 392 145
4	1.798 515 045 521 241	1.211 810 836 367 619
5	1.923 848 231 267 622	1.164 374 555 192 450
6	2.027 608 945 103 857	1.125 001 488 941 636
7	2.115 709 764 900 265	1.091 512 525 007 183
8	2.191 966 367 371 986	1.062 490 013 670 246
9	2.258 977 760 090 717	1.036 962 918 106 255
10	2.318 589 791 981 952	1.014 238 779 515 961
11	2.372 157 936 598 986	0.993 807 536 013 206

We solved these equations by seeking the solution of

$$(A_{T-1}(z) - A_T(z))(B_{T+1}(z) - B_T(z)) = (A_T(z) - A_{T+1}(z))(B_T(z) - B_{T-1}(z)),$$

which we call $z_c(T)$, and then found $\lambda(T)$ by back substitution. The results are shown in table 2.

We plotted (not shown) the estimates of $z_c(T)$, against various powers of $1/T$, and found a linear plot if we plotted against $1/T^2$. We extrapolated the estimates $z_c(T)$ for steadily increasing T values using the same Bulirsch–Stoer extrapolation method described above. Rapid convergence was observed, and we estimate $z_c = 0.379\,052\,28 \pm 0.000\,000\,01$. This is consistent with the limit found from our previous method described above, though not quite as precise.

We have similarly extrapolated the estimates of $\lambda(T)$, and find $\lambda \approx 0.382\,68$, compared to the expected value $\cos(3\pi/8) = 0.382\,682$.

4. Triangular lattice

We have also generated data for the triangular lattice in strips of widths up to and including 11. Using the best estimate [14] of the critical point, $z_c = 0.240\,917\,5745$, we show, in table 3, the values of $A_T(z_c)$ and $B_T(z_c)$ for each strip width. For the triangular lattice there are two edges incident upon the origin in a strip geometry and this complicates matters. To

simplify things, we start and finish our SAW *on* the boundary in the case of the triangular lattice, in order to avoid the complications that arise when including an incident edge. So the extra factor of z_c included in the definition of these amplitudes for the square and honeycomb lattice data is not present in the triangular lattice data.

As in the analysis of the square lattice data, we fitted successive pairs of values $(A_T(z_c), B_T(z_c))$ and $(A_{T+1}(z_c), B_{T+1}(z_c))$ for $T = 1, \ldots, 10$ to

$$1 = c_\alpha(T)A_T(z_c) + c_\beta(T)B_T(z_c),$$

and solved the associated linear equations for $c_\alpha(T)$ and $c_\beta(T)$.

To obtain precise estimates, we again applied the Bulirsch–Stoer extrapolation algorithm to the sequences $\{c_\alpha(T)\}$ and $\{c_\beta(T)\}$. Combining the results from these different algorithms, we estimate $c_\alpha = 0.201\,2028(3)$ and $c_\beta = 0.525\,770(3)$. Thus the ratio $c_\alpha/c_\beta = 0.382\,682(3)$. For the honeycomb lattice the corresponding ratio is $\cos(3\pi/8) = 0.382\,6834\ldots$, which (as we also saw for the square lattice) is close to, and probably equal to, the triangular lattice value.

Assuming the ratio $c_\alpha/c_\beta = \cos(3\pi/8)$ for the triangular lattice too, we extrapolated $\cos(3\pi/8)A_T(z_c) + B_T(z_c)$ for increasing values of T, using our standard suite of extrapolation algorithms and the Bulirsch–Stoer algorithm. We estimated the limit to be $1.901\,979 \pm 0.000\,001$. We then repeated the analysis described above for the square lattice data *mutatis mutandis* and found

$$1.901\,979 - \frac{0.1}{T^2} \approx \cos(3\pi/8)A_T(z_c) + B_T(z_c).$$

As remarked above, it has been proved [2] that $\lim_{T\to\infty} B_T(z_c) = B(z_c) = 0$. Thus, in the limit of infinite strip width, we find $1.901\,979 \approx \cos(3\pi/8)A(z_c)$, a prediction for the critical amplitude $A(z_c) \approx 4.970\,111$.

As for the square lattice case, we estimated the critical point z_c by extrapolating the intersection point of $\cos(3\pi/8)A_T(z) + B_T(z)$ and $\cos(3\pi/8)A_{T+1}(z) + B_{T+1}(z)$, called $z_c(T)$. One expects $\lim_{T\to\infty} z_c(T) = z_c$.

In this way, we estimated

$$z_c = 0.240\,917\,572 \pm 0.000\,000\,005$$

for the triangular lattice. This can be compared to the best series estimate, based on the analysis of very long polygon series $z_c(\mathrm{tr}) = 0.240\,917\,5745$ [14] with uncertainty in the last quoted digit.

4.1. T dependence of the generating functions $A_T(z_c)$ and $B_T(z_c)$

As for the honeycomb and square lattices, we expect $B_T(z_c) \sim \mathrm{const}/T^{1/4}$. We plotted estimates of the exponent

$$\mathrm{grad}B(T) = \log\left(\frac{B_T(z_c)}{B_{T-1}(z_c)}\right) \Big/ \log\left(\frac{T}{T-1}\right)$$

against $1/T^{0.85}$, which should approach $-1/4$, and were seen to do so. The figure was visually indistinguishable from the corresponding figure 6 for the square lattice, so is not shown.

Similarly, it follows from (8) that $\tilde{A}_T(z_c) = A_T(z_c) - a_0 \approx A_T(z_c) - 4.970\,11$ decays as $1/T^{1/4}$ as T tends to infinity. As we did for the square lattice case, we also confirmed this numerically.

Table 4. Estimates of $z_c(T)$ and $\lambda(T)$ for the triangular lattice.

T	$z_c(T)$	$\lambda(T)$
2	0.241 168 440 165 255	0.356 318 356 471 223
3	0.241 030 169 141 752	0.366 143 831 978 748
4	0.240 977 832 351 101	0.371 147 184 391 665
5	0.240 953 612 190 006	0.374 091 365 359 823
6	0.240 940 839 933 527	0.375 992 279 128 027
7	0.240 933 460 889 859	0.377 300 697 288 292
8	0.240 928 899 289 076	0.378 244 599 187 661
9	0.240 925 927 855 959	0.378 950 553 554 884
10	0.240 923 909 640 445	0.379 493 901 730 187

4.2. Alternative estimate of the critical point

In the previous section, we showed that, for the square lattice data, the simultaneous solution of the pair of equations

$$\lambda A_{T-1}(z) + B_{T-1}(z) - \lambda A_T(z) - B_T(z) = 0$$

and

$$\lambda A_T(z) + B_T(z) - \lambda A_{T+1}(z) - B_{T+1}(z) = 0$$

gives a sequence of estimates of $z_c(T)$ that converges to the critical point z_c. Similarly, the parameter λ converges to the ratio $c_\alpha/c_\beta = \cos(3\pi/8)$, where the equality is conjectural. We solved these equations using the triangular lattice data, by seeking the solution of

$$(A_{T-1}(z) - A_T(z))(B_{T+1}(z) - B_T(z)) = (A_T(z) - A_{T+1}(z))(B_T(z) - B_{T-1}(z)),$$

called $Z_c(T)$, and then found $\lambda(T)$ by back substitution. The results are shown in table 4.

We plotted (not shown) the estimates of $z_c(T)$, against various powers of $1/T$, and found a linear plot if we plotted against $1/T^2$. We analysed the sequences in precisely the same way as for the corresponding square lattice data, using the Bulirsch–Stoer algorithm. The merit of this method of estimating the critical point is that it makes no assumption about the value of λ, while the method of estimating the critical point described in section 4 assumes that $\lambda = \cos(3\pi/8)$. For the critical point we estimate $z_c = 0.240\,917\,575 \pm 0.000\,000\,005$. This is of comparable precision to our estimate given in section 4, but slightly less precise than the best series estimate [14] of $z_c = 0.240\,917\,5745$, with uncertainty in the last digit.

Thus this method is again seen to be a powerful one for estimating critical points, giving very good accuracy. We have similarly extrapolated the estimates of $\lambda(T)$, and find $\lambda \approx 0.382\,68$, compared to the expected value $\cos(3\pi/8) = 0.382\,682$, exactly as for the square lattice.

5. Enumeration of self-avoiding walks

The algorithm we use to enumerate SAWs on the square lattice builds on the pioneering work of Enting [7] who enumerated square lattice SAPs using the finite lattice method. More specifically, our algorithm is based in large part on the one devised by Conway, Enting and Guttmann [5] for the enumeration of SAWs. The details of our algorithm can be found in [13]. Below we shall only briefly outline the basics of the algorithm and describe the changes made for the particular problem studied in this work.

The generating function for a rectangle was calculated using transfer matrix (TM) techniques. The most efficient implementation of the TM algorithm generally involves

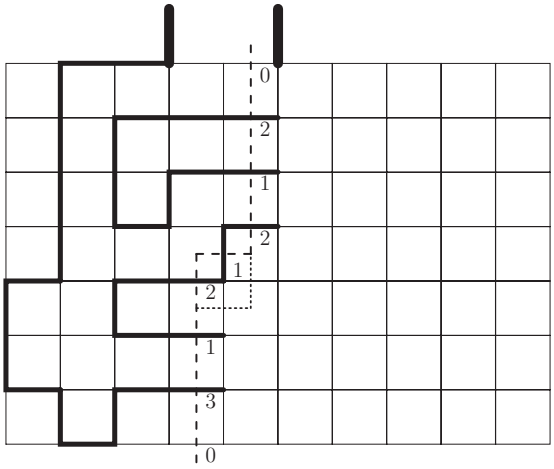

Figure 7. A snapshot of the boundary line (dashed line) during the transfer matrix calculation of type *A* configurations on a strip of size 7×10. SAWs are enumerated by successive moves of the kink in the boundary line, as exemplified by the position given by the dotted line, so that one vertex and two edges at a time are added to the strip. To the left of the boundary line, we have drawn an example of a partially completed SAW. The heavy lines at the top denotes the incoming and outgoing edges of the SAW.

bisecting the finite lattice with a boundary (this is just a line in the case of rectangles) and moving the boundary in such a way as to build up the lattice vertex by vertex as illustrated in figure 7. If we draw a SAW and then cut it by a line, we observe that the partial SAW to the left of this line consists of a number of loops connecting two edges (we shall refer to these as loop ends) in the intersection, and pieces which are connected to only one edge (we call these free ends). The other end of the free piece is an end point of the SAW so there are at most two free ends.

Each end of a loop is assigned one of the two labels depending on whether it is the lower end or the upper end of a loop. Each configuration along the boundary line can thus be represented by a set of edge states $\{\sigma_i\}$, where

$$\sigma_i = \begin{cases} 0 & \text{empty edge,} \\ 1 & \text{lower loop-end,} \\ 2 & \text{upper loop-end.} \\ 3 & \text{free end.} \end{cases} \tag{10}$$

If we read from the bottom to the top, the configuration or signature S along the intersection of the partial SAW in figure 7 is $S = \{031212120\}$. Since crossings are not permitted, this encoding uniquely describes which loop ends are connected.

A few changes to the algorithm described in [13] are required in order to enumerate the restricted SAWs we study here. Most importantly, the SAW must have a free end at the middle vertex of the top side of the strip. This is easily ensured by restricting the updating rules at this vertex (also signatures prior to passing this vertex can have at most one free end). Specifically, the middle vertex is reached when the TM boundary has been moved halfway through the strip. At this point the incoming edge to the left of the middle vertex is either empty, an upper loop-end or free. In the *empty* case, we have to insert a new free end (along either the horizontal or the vertical outgoing edge). In the *upper* case, the loop-end is terminated and the matching lower loop-end becomes a free end.

In the *free* case, the end is again terminated and all the edges connected to this free end form a SAW. However, this is only a valid configuration if all other edges are empty since otherwise we would form configurations with more than one component. Second, in enumerating SAWs of type A the second free end must lie in the top side of the rectangle; we chose to force the free end to lie to the left of the middle vertex and use symmetry to count all possible configurations. In counting bridges or SAWs of type B, the second free end must lie at the bottom of the strip. Third, in [13], the SAWs were forced to span the rectangle, that is touch all sides, but this restriction is lifted in this study.

The sum over all contributing graphs is calculated as the boundary is moved through the lattice. For each configuration of occupied or empty edges along the intersection, we maintain a generating function G_S for partial walks with signature S. In exact enumeration studies G_S would be a truncated two-variable polynomial $G_S(z)$, where z is conjugate to the number of steps.

In a TM update, each source signature S (before the boundary is moved) gives rise to a few new target signatures S' (after the move of the boundary line) and $n = 0, 1$ or 2 new edges are inserted leading to the update $G_{S'}(z) = G_{S'}(z) + z^n G_S(z)$. Once a signature S has been processed it can be discarded. In most studies, the calculations were done using integer arithmetic modulo several primes with the full integer coefficients reconstructed at the end using the Chinese remainder theorem. Here we are not really interested in the exact coefficients. This makes life a little easier for us since we can use real coefficients with the generating functions truncated at some maximal degree M. The calculations were carried out using quadruple (or 128-bit) floating-point precision (achieved in FORTRAN with the REAL(KIND=16) type declaration).

In our calculations we truncated $A_T(z)$ and $B_T(z)$ at degree $M = 1000$ and used strips of half-length $L = M$. These choices of M and L more than suffice to ensure that numerical errors are negligible as evidenced by the fact that when we solve (4) (with z_c replaced by z) to find z_c for the honeycomb lattice the estimate for z_c agrees with the exact value to at least 30 digits, that is, to within the numerical accuracy of the floating-point computation itself.

The computational complexity of the calculation required to obtain the number of walks in a strip of width T and length L can be easily estimated. Time (and memory) requirements are basically proportional to a polynomial in M and L times the maximal number of signatures, N_{Conf}, generated during the calculation. It is well established [12] that $N_{\text{Conf}} \propto 3^T$ so the algorithm has exponential computational complexity.

The transfer-matrix algorithm is eminently suited to parallel computations and here we used the approach first described in [12] and refer the interested reader to this publication for further detail. The bulk of the calculations for this paper were performed on the cluster of the NCI National Facility, which provides a peak computing facility to researchers in Australia. The NCI peak facility is a Sun Constellation Cluster with 1492 nodes in Sun X6275 blades, each containing two quad-core 2.93 GHz Intel Nehalem CPUs with most nodes having 3 GB of memory per core (24 GB per node). It took a total of about 1800 CPU hours to calculate $A_T(z)$ for T up to 15. The bulk of the time (almost 1250 h) was spent calculating $A_{15}(z)$. In this case, we used 48 processors and the split between actual calculations and communications was roughly 2 to 1 (with quite a bit of variation from processor to processor). Smaller widths can be done more efficiently in that communication needs are fewer and hence not as much time is used for this task.

On a technical issue we note that quad precision is not a supported data type in the MPI standard. So in order to pass messages containing the generating functions, we used the MPI data type MPI-BYTE with each coefficient then having a length of 16 bytes.

The algorithm used for the triangular lattice is quite similar. The triangular lattice is represented as a square lattice with additional edges along one of the main diagonals. This poses an immediate problem since a boundary line drawn as in figure 7 would intersect $2T$ edges thus greatly increasing the number of possible signatures. In this case it is more efficient to draw the boundary line through the vertices of the lattice. We then again have T intersections, however a vertex may be in an additional state since a partial SAW can touch the boundary line without crossing it (see [14] for further details). The upshot is that the computational complexity grows exponentially as 4^T.

6. Conclusion

We started this study in order to consider to what extent, in some ill-defined sense, does there exist a parafermionic operator applicable to SAWs on the square and triangular lattices. For honeycomb lattice SAWs, (8) is an identity. For the square and triangular lattices we found, experimentally, that for walks in a strip of width T on the square lattice

$$1.024\,966(1 - 0.14/T^2) \approx \cos(3\pi/8)A_T(z_c) + B_T(z_c), \tag{11}$$

while for the triangular lattice the corresponding result is

$$1.901\,979(1 - 0.1/T^2) \approx \cos(3\pi/8)A_T(z_c) + B_T(z_c). \tag{12}$$

Since $B_T(z_c) \to 0$ as $T \to \infty$, it follows that in the same limit $A_T(z_c) \to a_0$, where the numerical value of $a_0 = 1/\cos(3\pi/8)$ for the honeycomb lattice, $a_0 \approx 1.024\,966/\cos(3\pi/8)$ for the square lattice, and $a_0 \approx 1.901\,979/\cos(3\pi/8)$ for the triangular lattice. We provided numerical support for the conjecture that $B_T(z_c) \sim \text{const}/T^{1/4}$ as $T \to \infty$, and hence that $A_T(z_c) - a_0 \sim \text{const}/T^{1/4}$ also. Finally we show how the existence of equations (8), (11) and (12) suggests a powerful numerical method to estimate the critical point. In that way we found z_c exactly for the honeycomb lattice, and estimated $z_c = 0.379\,052\,2775(5)$ for the square lattice and $z_c = 0.240\,917\,573(5)$ for the triangular lattice.

It has been pointed out to the authors by Cardy that in the scaling limit, all two-dimensional SAW models are given by the same conformal field theory. Since it is known that for one of these models (i.e. honeycomb lattice SAW) the critical point can be found by requiring certain contour integrals to vanish (i.e. when summing (1) over a region of the lattice), it follows that in the scaling limit the same must be true for all two-dimensional SAWs. This is entirely consistent with our observations and the relations (11) and (12).

Acknowledgments

We thank Jan de Gier and John Cardy for many discussions that aided our understanding. This work was supported by an award under the Merit Allocation Scheme on the NCI National Facility at the ANU and was supported under the Australian Research Council's Discovery Projects funding scheme in grants to AJG and IJ. NRB was supported by the ARC Centre of Excellence for Mathematics and Statistics of Complex Systems (MASCOS).

References

[1] Barber M N and Hamer C J 1982 Extrapolation of sequences using a generalized epsilon-algorithm *J. Aust. Math. Soc.* B **23** 229–40

[2] Beaton N R, de Gier J and Guttmann A J 2011 The critical fugacity for surface adsorption of SAW on the honeycomb lattice is $1 + \sqrt{2}$ arXiv:1109.1234

[3] Bulirsch R and Stoer J 1964 Fehlerabschätzungen und extrapolation mit rationalen funktionen bei verfahren vom Richardson-typus *Numer. Math.* **6** 413–27
[4] Caracciolo S, Guttmann A J, Jensen I, Pelissetto A, Rogers A N and Sokal A D 2005 Correction-to-scaling exponents for two-dimensional self-avoiding walks *J. Stat. Phys.* **120** 1037–100
[5] Conway A R, Enting I G and Guttmann A J 1993 Algebraic techniques for enumerating self-avoiding walks on the square lattice *J. Phys. A: Math. Gen.* **26** 1519–34
[6] Duminil-Copin H and Smirnov S 2010 The connective constant of the honeycomb lattice equals $\sqrt{2+\sqrt{2}}$ arXiv:1007.0575
[7] Enting I G 1980 Generating functions for enumerating self-avoiding rings on the square lattice *J. Phys. A: Math. Gen.* **13** 3713–22
[8] Guttmann A J 1989 Analysis of coefficients *Phase Transitions and Critical Phenomena* vol 13 ed C Domb and J L Lebowitz (London: Academic) pp 1–234
[9] Guttmann A J and Torrie G M 1984 Critical behaviour at an edge for the SAW and Ising model *J. Phys. A: Math. Gen.* **17** 3539–52
[10] Ikhlef Y and Cardy J 2009 Discretely holomorphic parafermions and integrable loop models *J. Phys. A: Math. Theor.* **42** 102001
[11] Jensen I and Guttmann A J 1999 Self-avoiding polygons on the square lattice *J. Phys. A: Math. Gen.* **32** 4867–76
[12] Jensen I 2003 A parallel algorithm for the enumeration of self-avoiding polygons on the square lattice *J. Phys. A: Math. Gen.* **36** 5731–45
[13] Jensen I 2004 Enumeration of self-avoiding walks on the square lattice *J. Phys. A: Math. Gen.* **37** 5503–24
[14] Jensen I 2004 Self-avoiding walks and polygons on the triangular lattice *J. Stat. Mech.* P10008
[15] Lawler G, Schramm O and Werner W 2004 On the scaling limit of planar self-avoiding walk *Fractal Geometry and Applications: A Jubilee of Benoit Mandelbrot: Part 2 (Proc. Symp. Pure Math.* vol 72*)* (Providence, RI: AMS) pp 339–64
[16] Monroe J L 2002 Extrapolation and the Bulirsch–Stoer algorithm *Phys. Rev.* E **65** 066116
[17] Nienhuis B 1982 Exact critical point and critical exponents of O(n) models in two dimensions *Phys. Rev. Lett.* **49** 1062–5
[18] Janse van Rensburg E J, Orlandini E and Whittington S G 2006 Self-avoiding walks in a slab: rigorous results *J. Phys. A: Math. Gen.* **39** 13869–902
[19] Smirnov S 2010 Discrete complex analysis and probability *Proc. Int. Congress of Mathematicians (ICM) (Hyderabad, India)* pp 565–621 (arXiv:1009.6077)
[20] Cardy J 2011 private communication